Development and Validation of Passive Yaw in the Open-Source WEC-Sim Code

Preprint

David Ogden,[1] Jennifer van Rij,[1] Yi-Hsiang Yu,[1]
Nathan Tom,[1] Dominic D. Forbrush,[2] and Kelley Ruehl[2]

1 National Renewable Energy Laboratory
2 Sandia National Laboratories

Presented at the ASME 2020 39th International Conference on Ocean, Offshore and Artic Engineering
August 3–7, 2020

NREL is a national laboratory of the U.S. Department of Energy
Office of Energy Efficiency & Renewable Energy
Operated by the Alliance for Sustainable Energy, LLC

This report is available at no cost from the National Renewable Energy Laboratory (NREL) at www.nrel.gov/publications.

Contract No. DE-AC36-08GO28308

Conference Paper
NREL/CP-5000-76304
November 2020

Development and Validation of Passive Yaw in the Open-Source WEC-Sim Code

Preprint

David Ogden,[1] Jennifer van Rij,[1] Yi-Hsiang Yu,[1]
Nathan Tom,[1] Dominic D. Forbrush,[2] and Kelley Ruehl[2]

1 National Renewable Energy Laboratory
2 Sandia National Laboratories

Suggested Citation
Ogden, David, Jennifer van Rij, Yi-Hsiang Yu, Nathan Tom, Dominic D. Forbrush, and Kelley Ruehl. 2020. *Development and Validation of Passive Yaw in the Open-Source WEC-Sim Code: Preprint*. Golden, CO: National Renewable Energy Laboratory. NREL/CP-5000-76304. https://nrel.gov/docs/fy21osti/76304.pdf.

NREL is a national laboratory of the U.S. Department of Energy
Office of Energy Efficiency & Renewable Energy
Operated by the Alliance for Sustainable Energy, LLC

This report is available at no cost from the National Renewable Energy Laboratory (NREL) at www.nrel.gov/publications.

Contract No. DE-AC36-08GO28308

Conference Paper
NREL/CP- 5000-76304
November 2020

National Renewable Energy Laboratory
15013 Denver West Parkway
Golden, CO 80401
303-275-3000 • www.nrel.gov

NOTICE

This work was authored in part by the National Renewable Energy Laboratory, operated by Alliance for Sustainable Energy, LLC, for the U.S. Department of Energy (DOE) under Contract No. DE-AC36-08GO28308. Funding provided by U.S. Department of Energy Office of Energy Efficiency and Renewable Energy Water Power Technologies Office. The views expressed herein do not necessarily represent the views of the DOE or the U.S. Government. The U.S. Government retains and the publisher, by accepting the article for publication, acknowledges that the U.S. Government retains a nonexclusive, paid-up, irrevocable, worldwide license to publish or reproduce the published form of this work, or allow others to do so, for U.S. Government purposes.

Cover Photos by Dennis Schroeder: (clockwise, left to right) NREL 51934, NREL 45897, NREL 42160, NREL 45891, NREL 48097, NREL 46526.

DEVELOPMENT AND VALIDATION OF PASSIVE YAW IN THE OPEN-SOURCE WEC-SIM CODE

Dominic D. Forbush *
Kelley Ruehl
Sandia National Laboratories
Albuquerque, New Mexico 87123
Email: dforbus@sandia.gov

David Ogden
Jennifer van Rij
Yi-Hsiang Yu
Nathan Tom
National Renewable Energy Laboratory
18200 CO-128
Boulder, Colorado 80303

ABSTRACT

A passive yaw implementation is developed, validated, and explored for WEC-Sim, an open-source wave energy converter modeling tool that works within MATLAB/Simulink. The Reference Model 5 (RM5) is selected for this investigation, and a WEC-Sim model of the device is modified to allow yaw motion. A boundary element method (BEM) code was used to calculate the excitation force coefficients for a range of wave headings. An algorithm was implemented in WEC-Sim to determine the equivalent wave heading from a body's instantaneous yaw angle and interpolate the appropriate excitation coefficients to ensure the correct time-domain excitation force. This approach is able to determine excitation force for a body undergoing large yaw displacement. For the mathematically simple case of regular wave excitation, the dynamic equation was integrated numerically and found to closely approximate the results from this implementation in WEC-Sim. A case study is presented for the same device in irregular waves. In this case, computation time is increased by 32x when this interpolation is performed at every time step. To reduce this expense, a threshold yaw displacement can be set to reduce the number of interpolations performed. A threshold of 0.01^o was found to increase computation time by only 22x without significantly affecting time-domain results. Similar amplitude spectra for yaw force and displacements are observed for all threshold values less than 1^o, for which computation time is only increased by 2.2x.

INTRODUCTION

Extracting energy from ocean waves presents technical and practical challenges. Accurately modeling the dynamic response of a wave energy converter (WEC) prototype can advise design decisions and improve confidence in computer models of device physics. The Wave Energy Converter Simulator (WEC-Sim) is an open-source blockset (and support scripts) that works within MATLAB/Simulink using the multibody dynamics solver Simscape Multibody. WEC-Sim allows time-domain modeling of a user-specified WEC in operational and extreme waves. WEC-Sim is jointly developed by Sandia National Laboratories and the National Renewable Energy Laboratory through the Water Power Technologies Office of the U.S. Department of Energy [1] and is periodically validated against other codes and experimental data [2], [3], [4].

Since its release in 2014, updates to the WEC-Sim code have been driven by the modeling needs of the industry and research community, often submitted through the WEC-Sim GitHub issue page [1]. WEC-Sim development has built upon potential flow modeling approaches by incorporating additional fluid and device physics of particular importance to WECs such as the inclu-

*Address all correspondence to this author.

sion of viscosity, interaction between WEC bodies [5], weakly non-linear wave excitation and buoyancy [6], and flexible control implementations [7], [8], [9]. WEC-Sim is thus a mid-fidelity time-domain model and maintains a substantially smaller computational expense than high-fidelity computational fluid dynamics models by eschewing direct attempts to solve the Navier-Stokes equations [10].

This paper details the development and validation of the passive yaw implementation in the WEC-Sim code. Like passive yaw for wind turbines, passive yaw for WECs refers to the wave force acting on the body to hydrodynamically adjust the WEC's yaw orientation relative to the incident waves. This represents an extension to the small-amplitude motion assumptions presumed by linear potential flow solution methods. The implementation is first validated using the mathematically simple case of a yawing oscillating flap device in regular waves. A case study demonstrating the utility of the feature is then presented for a more complex wave state.

IMPLEMENTATION

WEC-Sim models WEC dynamics in the time domain by integrating the Cummins time-domain impulse-response formulation in 6 degrees of freedom [11]

$$m\ddot{X} = F_{exc}(t) + F_{rad}(t) + F_{pto}(t) + F_v(t) + F_{ME}(t) + F_B(t) + F_m(t) \quad (1)$$

where $\ddot{X}$ is the translational and rotational acceleration vector of the device, m is the inertia matrix (6 x 6), and the remaining terms are force/torque vectors (6 x 1) arising from distinct hydrodynamic components: F_{exc} is caused by wave excitation, F_{rad} is caused by wave radiation, F_{pto} is caused by the power takeoff (PTO), F_v is caused by viscous damping, F_{ME} captures additional damping related to Morison elements [1], F_B is caused by hydrostatics/buoyancy, and finally, F_m is the force/torque vector caused by mooring forces.

Initial Implementation

Excitation force exerted on the WEC depends on the direction, magnitude, and frequency of the incident wave field. Generally,

$$F_{exc} = \sum_{1}^{N} \eta(t) f_{exc}(\omega, \beta_0) \quad (2)$$

where η is a time-dependent N x 1 vector of wave height in each of N frequency bins, defined by frequencies ω, and f_{exc} is a complex 6 x N matrix of excitation coefficients for a given WEC relative yaw displacement β.

$$\beta = \theta - \psi \quad (3)$$

where θ is the incident wave direction (degrees), and ψ is the device yaw position. In Eq. 2, β_0 implies the initial β in the simulation, where time $t = 0$. For regular waves, which are monochromatic, Eq. 2 simplifies because there is only excitation at a single frequency (i.e., $N = 1$).

These excitation coefficients are provided by a frequency-domain boundary element method (BEM) solver and are an input to the WEC-Sim model. In the original implementation, f_{exc} were taken at a single β, based on the WEC initial position and wave heading. This is adequate to model axisymmetric or nearly axisymmetric devices (for which f_{exc} is a weak function of β) or devices that undergo small yaw displacements but yield modeling errors in other cases. A physical device might passively yaw because of changes in excitation coefficients resulting from changing relative yaw position. However, this phenomenon will not be accurately modeled by the initial implementation of WEC-Sim because the set of f_{exc} coefficients does not change with β. It is this case that is of interest for this study.

Passive Yaw Implementation

Because only excitation force coefficients vary explicitly with wave direction, and by extension relative yaw angle, it is sufficient to revise Eq. 2 to use f_{exc} coefficients that vary with instantaneous relative yaw position β.

$$F_{exc} = \sum_{1}^{N} \eta(t) f_{exc}(\omega, \beta) \quad (4)$$

.

Because WEC-Sim depends on BEM estimates of f_{exc}, modeling accuracy will be enhanced only if f_{exc} are populated for multiple values of β bounding the range of device motion. However, because the range of device yaw motion ψ is not known *a priori*, it is most prudent to calculate f_{exc} over a broad range of θ (Eq. 3), such that the BEM-provided f_{exc} becomes 6 x N x K, where K is the number of θ values at which a BEM calculation was performed. The appropriate values of f_{exc} (Eq. 4) can be determined at a given instant by linear interpolation in β over all N frequencies (for irregular waves) or over a single frequency (for regular waves) provided that two exceptions are handled.

Firstly, by convention, yaw angles are between -180^o and 180^o in WEC-Sim, but, depending on the specific code used, BEM outputs can have various ranges (e.g., 0^o to 360^o). BEM

outputs thus must be wrapped to 180^o to ensure accurate calculation. Secondly, because naive linear interpolation is used, the minimum and maximum BEM outputs must be wrapped when β falls outside of the range of θ calculated by BEM. In these instances, the appropriate bound of ψ is adjusted to ψ_{new} for the interpolation as:

$$\psi_{new} = min(\psi) + 360; \beta > max(\psi) \tag{5}$$
$$\psi_{new} = max(\psi) - 360; \beta < min(\psi) \tag{6}$$

.

This also handles the periodicity of f_{exc} in β with a period of 360^o.

Finally, for particularly large values of N, the number of operations completed at each simulation step can increase markedly because of this interpolation. However, especially for small simulation time steps, the change in yaw displacement from the previous time step is likely to be so small as to be negligible in terms of the effect on f_{exc}, implying that interpolation is increasing the computation time without substantially improving accuracy. To address this, a user-specified threshold $\Delta\beta$ (degrees) was implemented such that interpolation will only be performed at time step n if significant relative yaw displacement has occurred.

$$\Delta\beta < |\beta_n - \beta_{n_l}| \tag{7}$$

where n_l is the time step at which the last interpolation occurred, and vertical bars imply an absolute value. Further, because a certain population of θ values have been pre-calculated by the BEM code, interpolation is similarly unnecessary at time steps for which $\Delta\beta < |min(\beta_n - \theta)|$ wherein the pre-calculated values of f_{exc} at the nearest θ are used.

Coordinate Transformation

WEC-Sim computes the system's equations of motion (Eq. 1) in a fixed global reference frame; the force vectors on the right-hand side of this equation must be provided in the same frame. As WEC-Sim is based on linear potential flow theory, small amplitude motion about a body's equilibrium position is typically assumed in the time-domain simulations. However, as the passive yaw feature may permit large displacements in yaw, some transformations are necessary to ensure the force vectors are calculated and returned in the correct reference frame.

The $F_{exc}(t)$ vector returned by Eq. 4 accounts for the body's global yaw angle and the wave heading to determine the correct relative wave heading. But the $f_{exc}(\omega, \beta)$ vectors have been computed for the body's zero-yaw position (i.e., $\psi = 0$) for various wave headings and do not account for variations in the body's global yaw angle, $\psi(t)$. Hence, $F_{exc}(t)$ must be transformed about the z-axis by the body's global yaw angle to obtain the excitation force vector in the global frame.

$$F_{exc,global} = \mathbf{R}_{yaw} F_{exc,local} \tag{8}$$

where

$$\mathbf{R}_{yaw} = \begin{bmatrix} \cos(\psi) & -\sin(\psi) & 0 \\ \sin(\psi) & \cos(\psi) & 0 \\ 0 & 0 & 1 \end{bmatrix} \tag{9}$$

Similarly, the hydrostatic and radiation forces, $F_B(t)$ and $F_{rad}(t)$, are computed using coefficients calculated for the body's equilibrium position and do not account for large displacements in yaw. Therefore, the kinematic variables passed to these functions must be transformed from the global frame into the body's local frame. The local translational kinematic vectors can be obtained using the transpose of $\mathbf{R}_{yaw}$.

$$x_{local} = \mathbf{R}_{yaw}^T x_{global} \tag{10}$$
$$\dot{x}_{local} = \mathbf{R}_{yaw}^T \dot{x}_{global} \tag{11}$$
$$\ddot{x}_{local} = \mathbf{R}_{yaw}^T \ddot{x}_{global}. \tag{12}$$

In WEC-Sim, rotational kinematic variables are expressed in the Tait-Bryan x-y-z extrinsic convention: ϕ, θ, ψ (roll, pitch, yaw). To determine the local rotational kinematic vectors, first the body's global rotation matrix is obtained from the Tait-Bryan angles.

$$\mathbf{R}_{global} = \begin{bmatrix} \mathrm{c}(\theta)\mathrm{c}(\psi) & -\mathrm{c}(\theta)\mathrm{s}(\psi) & \mathrm{s}(\theta) \\ \mathrm{c}(\phi)\mathrm{s}(\psi) + \mathrm{s}(\phi)\mathrm{s}(\theta)\mathrm{c}(\psi) & \mathrm{c}(\phi)\mathrm{c}(\psi) - \mathrm{s}(\phi)\mathrm{s}(\theta)\mathrm{s}(\psi) & -\mathrm{s}(\phi)\mathrm{c}(\theta) \\ \mathrm{s}(\phi)\mathrm{s}(\psi) - \mathrm{c}(\phi)\mathrm{s}(\theta)\mathrm{c}(\psi) & \mathrm{s}(\phi)\mathrm{c}(\psi) + \mathrm{c}(\phi)\mathrm{s}(\theta)\mathrm{s}(\psi) & \mathrm{c}(\phi)\mathrm{c}(\theta) \end{bmatrix} \tag{13}$$

where c and s are short-hand for the cosine and sine functions, respectively, adopted here for readability. Now the difference between $\mathbf{R}_{global}$ and $\mathbf{R}_{yaw}$ yields the body's orientation minus its global yaw displacement (i.e., in a local frame).

$$\mathbf{R}_{local} = \mathbf{R}_{yaw}^T \mathbf{R}_{global} \tag{14}$$

From $\mathbf{R}_{local}$, the Tait-Bryan angles in the local frame are:

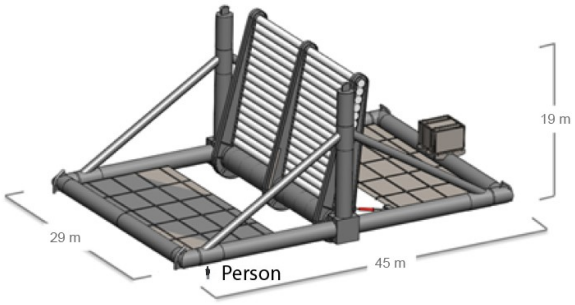

FIGURE 1. RENDERING OF THE RM5 DEVICE.

$$\phi = atan2(-\mathbf{R}_{local}[2,3], \mathbf{R}_{local}[3,3]) \quad (15)$$
$$\theta = asin(\mathbf{R}_{local}[1,3]) \quad (16)$$
$$\psi = atan2(-\mathbf{R}_{local}[1,2], \mathbf{R}_{local}[1,1]) \quad (17)$$

where the bracketed values are the row and column indices of the specified matrix. The same process is applied to obtain rotational velocity and acceleration in a local frame. These variables are then passed to WEC-Sim's hydrostatic and radiation functions, which calculate $F_B(t)$ and $F_{rad}(t)$ in a local frame. Hence, the same transformation as shown in Eq. 8 must be performed on these vectors.

$$F_{B,global} = \mathbf{R}_{yaw} F_{B,local} \quad (18)$$
$$F_{rad,global} = \mathbf{R}_{yaw} F_{rad,local} \quad (19)$$

noting that $\mathbf{R}_{yaw}$ is an orthogonal matrix.

VALIDATION

A simplified version of the Reference Model 5 (RM5) oscillating surge device was selected for validation of the passive yaw implementation [12]. The RM5 is a shallow-water flap-type pitching device fixed to the sea bed (Figure 1).

For this validation study, the device was fixed in pitch and instead allowed to oscillate about a central vertical axis in yaw. While this is clearly impractical for energy extraction, this greatly simplifies device dynamics and allows the WEC-Sim implementation (Figure 2) to be compared to an intuitive numerical solution. Mooring forces F_m and buoyancy forces F_B do not act in the yaw direction. Further, we neglect additional viscous losses F_v and oscillatory forcing from Morison's equation, F_{ME}. Thus, Eq. 1 simplifies to:

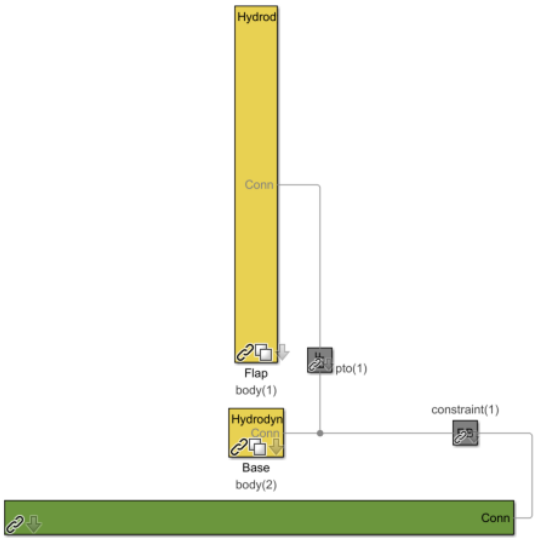

FIGURE 2. WEC-SIM MODEL OF THE SIMPLIFIED RM5 DEVICE. THE CONSTRAINT FIXES THE BASE TO THE SEA FLOOR, WHILE THE PTO ALLOWS YAW MOTION BETWEEN THE BASE AND FLAP.

$$m\ddot{X} = F_{exc}(t) + F_{rad}(t) + F_{pto(t)} \quad (20)$$

To further simplify dynamics, the device was simulated in a regular wave field, and F_{pto} was prescribed as linear damping. At this single frequency, the inertial and viscous components of F_{rad} are constant and can be summed with the static inertia m and F_{pto}, respectively. Finally, as the device is only allowed to actuate in yaw, only the yaw degree of freedom is considered. Under these conditions, the dynamics simplify to

$$M\ddot{x} + D\dot{x} = f_{exc}(\omega_0, \beta) A \cos \omega_0 t \quad (21)$$

where M is the combined (added and static) inertias in yaw, D is the combined (radiation and PTO) damping, and x refers to the yaw displacement. The exciting wave has an amplitude of A (m) and a frequency of ω_0 (rad/s), at which all relevant parameters have been evaluated (Table 1).

The BEM code WAMIT was used to estimate f_{exc} over a range of 0^o to 350^o at 10^o intervals at ω_0 [13]. Figure 3 shows that the yaw excitation coefficient varies significantly in a sinusoidal manner with a repeat period of 180^o, which is expected given the symmetry of the flap.

TABLE 1. PARAMETER VALUES USED IN VALIDATION SIMULATION.

D	2.905e5	N-m-s
M	2.940e7	kg m^2
ω_o	7.854e-1	rad/s
A	1.250	m

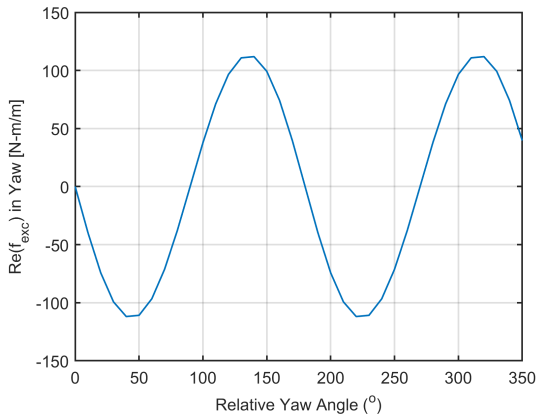

FIGURE 3. BEM-ESTIMATED EXCITATION COEFFICIENTS FOR THE RM5 DEVICE IN YAW FOR A WAVE PERIOD OF 8 SECONDS.

If BEM data are approximated by their nearest sinusoid [noting that, at this frequency, $\Re f_{exc}(\omega_o) >> \Im f_{exc}(\omega_o)$], then Eq. 21 becomes

$$M\ddot{x} + D\dot{x} = B\sin(\frac{2\psi\pi}{180})A\cos\omega_0 t$$

where B is one-half the range of the excitation coefficients at this frequency. This equation has the recognizable form of a decaying oscillator with amplitude-modulated forcing. Thus, the solution can be anticipated to be the superposition of the amplitude-modulation frequency and the wave-excitation frequency. Because of the simplicity of this hydrodynamic model, this can be integrated numerically (e.g., using MATLAB ODE45) as a close approximation to the WEC-Sim model. An initial yaw position of 0^o and a yaw velocity of $0^o/s$ were used as initial conditions, with an incident wave direction of 10^o and an integration time step of 0.01 s.

We see that the WEC-Sim model agrees closely with the ODE45 approximation and has the expected features (Figure 4). The longer period oscillation ($\sim$ 75 s) corresponds to the decay period of the yawing flap, while the shorter period oscillations (8 s) are the direct wave excitation. In accordance with physical intuition, the relative flap yaw goes to zero over time, aligning

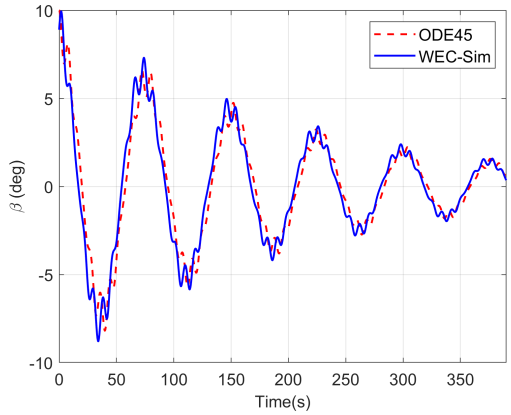

FIGURE 4. A COMPARISON OF THE PASSIVE YAW IMPLEMENTATION IN WEC-SIM WITH AN ODE45 APPROXIMATION.

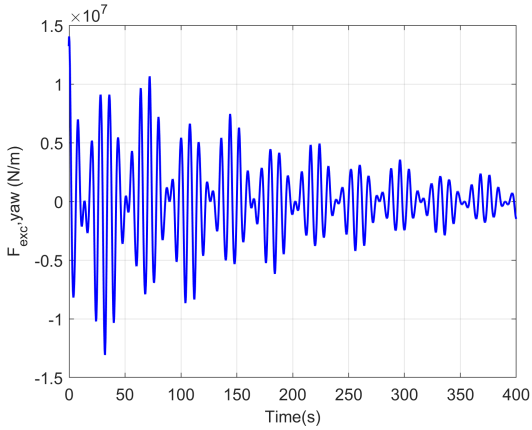

FIGURE 5. YAW EXCITATION FORCE AS DETERMINED BY THE WEC-SIM PASSIVE YAW IMPLEMENTATION.

with the wave direction. The excitation force in yaw calculated by WEC-Sim is also plotted as a check of the implementation because the passive yaw modifications directly affect F_{exc} (Figure 5). The excitation force is smooth and continuous, suggesting that the interpolation scheme utilized for f_{exc} coefficients does not cause numerical stability issues.

By comparison, the initial implementation (without passive yaw adjustment of f_{exc}) was run under otherwise identical conditions (Table 1). Yaw position results for this run are shown as Figure 6. There is no decay of the relative yaw position to align with the incident wave, only an oscillation at the frequency of wave excitation. This highlights the limitations of the initial implementation and the need for adjustment of f_{exc} under large yaw displacements.

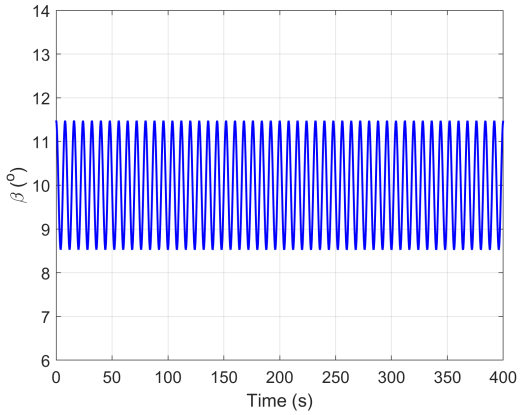

FIGURE 6. YAW POSITION RESULT OF THE INITIAL IMPLEMENTATION.

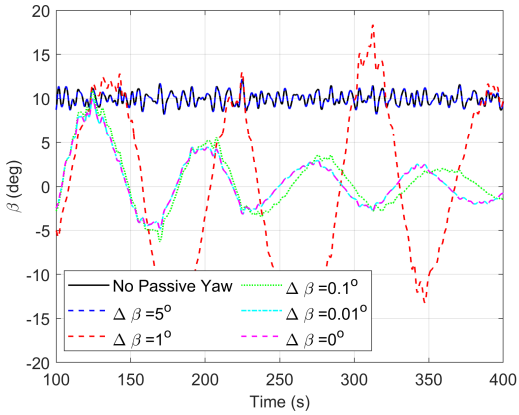

FIGURE 7. POSITION OUTPUT WITH AND WITHOUT PASSIVE YAW FOR SEVERAL VALUES OF $\Delta\beta$ UNDER IRREGULAR WAVE EXCITATION. NOTE THAT $\Delta\beta = 0.01^o$ IS OVERLAID BY $\Delta\beta = 0^o$, AND NO-PASSIVE YAW IS OVERLAID BY $\Delta\beta = 5^o$.

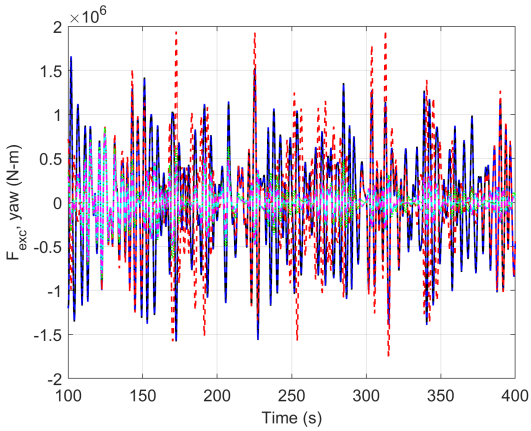

FIGURE 8. YAW EXCITATION OUTPUT WITH AND WITHOUT PASSIVE YAW FOR SEVERAL VALUES OF $\Delta\beta$ UNDER IRREGULAR WAVE EXCITATION. COLORS MAP IN THE SAME MANNER AS FIGURE 7.

CASE STUDY

The passive yaw implementation was investigated under the more mathematically complex case of irregular waves for which the more general Eq. 20 describes system dynamics. WAMIT was run again for ω, ranging from 0.04 rad/s to 20 rad/s in steps of 0.04 rad/s, to provide estimates of f_{exc} over the range of yaw angles. This test was conducted with and without passive yaw correction for five different values of $\Delta\beta$ to explore the effect on output and computation time (Eq. 7). A Pierson-Moskowitz spectrum with a significant wave height of 2.5 m and a peak period of 8 s was selected for study, as yaw excitation coefficients at this period are large for the modified RM5 device [14] [1]. To prevent large transients related to the initialization of the model, the amplitude of the simulated wave field was linearly increased to the prescribed level over 100 s, and the device was simulated for 400 s. Results are shown for the last 300 s of the test, after the wave amplitude reached the prescribed value.

The outputs of position and excitation force in yaw are considered in the time (Figures 7 and 8) and frequency domains (Figures 9 and 10). Amplitude spectra were determined from the detrended time-domain output by taking the absolute value of twice the Fourier transform over the positive frequencies. The median, range, and variance are also determined for each quantity to consider statistical agreement (Table 2).

Significantly different dynamics are observed between the passive yaw and initial implementations in the time domain (Figure 7). Cases for which f_{exc} interpolation occurs predict a much larger range of flap positions, while non-interpolating cases stay near the initial yaw angle of 10^o (Table 2). Dynamics from the largest $\Delta\beta$ run are identical to the initial implementation: Because β never exceeds 5^o, interpolation to update f_{exc} is never actually performed. In contrast, computation time increases markedly for $\Delta\beta = 0^o$ over $\Delta\beta = 0.01^o$ because of interpolation occurring at every time step, while the time-domain results are nearly indiscernible (Table 2, Figure 7). Time-domain results for $\Delta\beta = 0.1^o$ are also characteristically similar, showing a gradual decay to $\beta = 0$. However, time-domain results for $\Delta\beta = 1$ do not show this decay. A large disagreement for $\Delta\beta$ values above a certain size is unsurprising, as the integration of Eq. 20 will depend on non-constant F_{exc}, implying that small differences at each time step from differences in interpolated instantaneous excitation coefficients will propagate forward through the simulation. The $\Delta\beta$ values for which these characteristically distinct dynamics occur were found to also depend on the phase realization of the exciting irregular wave (not shown). This suggests that a non-zero, but small, value of $\Delta\beta$ is the ideal selection to avoid the negative

TABLE 2. STATISTICAL SUMMARY OF CASE STUDY SIMULATION.

	No-Passive Yaw	$\Delta\beta = 5^o$	$\Delta\beta = 1^o$	$\Delta\beta = 0.1^o$	$\Delta\beta = 0.01^o$	$\Delta\beta = 0^o$
Computation Time (s)	107	201	227	345	1,416	3,422
Median ψ (^{o})	0.04	0.04	9.46	9.30	9.67	9.67
Variance ψ (^{o2})	0.50	0.50	96.53	11.53	9.40	9.30
Range ψ (^{o})	4.03	4.03	34.87	17.14	14.83	14.75
Median F_{exc}, yaw (N-m)	3.78e4	3.78e4	-0.91	24.14	-893.53	-885.84
Variance F_{exc}, yaw (N-m)^2	3.51e11	3.51e11	3.11e11	3.79e10	3.14e10	3.11e10
Range F_{exc}, yaw (N-m)	3.24e6	3.24e6	3.27e6	1.72e6	1.59e6	1.59e6

effects of either extreme. Several values should be attempted for several phase realizations (in the case of irregular waves) to ensure that the output dynamics are reasonable.

Similar conclusions can be drawn from inspection of time-domain force outputs (Figure 8). The largest force peaks correspond to $\Delta\beta = 1^o$, indicating that although interpolation was occurring, it was too infrequent to capture the decaying trend present for smaller values of $\Delta\beta$.

The position amplitude spectra indicates that all but the largest $\Delta\beta$ value (for which no interpolation occurred) are capturing similar physics (Figure 9). When no interpolation occurs, only the frequencies corresponding to the wave excitation band show elevated amplitudes. In all interpolating cases, however, amplitudes at low frequencies are elevated, capturing the passive yaw motion. High frequencies (those greater than the largest exciting wave frequency) are also elevated. The frequency content of these interpolating cases are all similar over the frequencies of interest, though $\Delta\beta = 1$ [dynamically distinct (Figure 7)] shows elevated frequency content relative to all other cases. This suggests that adequate frequency domain agreement could potentially be obtained for larger values of $\Delta\beta$ than those yielding time-domain agreement.

The force amplitude spectra (Figure 10) cases for which interpolation occurs are less distinct from the cases without passive yaw than the position spectra. Excluding $\Delta\beta = 1^o$, all interpolating cases show generally reduced amplitudes across all frequencies. This is unsurprising, as the magnitude of force excitation coefficients are reduced with the relative yaw angle (Figure 3), and all of these cases are decaying in the time domain. Conversely, $\Delta\beta = 1^o$, which sees the largest relative yaw angles, has the highest amplitudes of any case at low frequencies but otherwise behaves similarly to the baseline no-passive yaw case.

Inspecting Table 2, the computation time increases with decreasing $\Delta\beta$. Even for $\Delta\beta = 5^o$, where no interpolation occurred, computation time is nearly 2x of that for no-passive yaw. Median yaw position is zero for cases without interpolation and approaching the incident wave heading (10^o) for all others. For

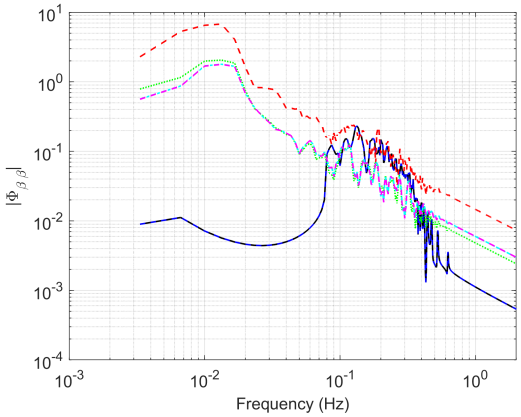

FIGURE 9. AMPLITUDE SPECTRA OF POSITION WITH AND WITHOUT PASSIVE YAW FOR SEVERAL VALUES OF $\Delta\beta$ UNDER IRREGULAR WAVE EXCITATION. COLORS MAP IN THE SAME MANNER AS FIGURE 7.

$\Delta\beta = 1^o$, the variance of range and position is significantly overestimated: The variance and range of the no-passive yaw case is a more accurate estimate. In all cases, the median force should be near zero. Relative to the range of forces experienced, this is true, though all interpolating cases are nearer to zero than no-passive yaw. Similarly, the variance of excitation force is reduced by an order of magnitude for all interpolating cases except $\Delta\beta = 0$.

Collectively, this suggests that selection of $\Delta\beta$ should consider simulation objectives. If time-domain sensitive quantities are under investigation, for instance, for the maximum loads experienced for a specific excitation time series, then small values of $\Delta\beta$ must be used. However, study objectives pertaining only to frequency-domain or statistical metrics can be modeled accurately at larger values of $\Delta\beta$. It is insufficient to merely show that $\Delta\beta$ is sufficiently small such that interpolation is occurring. Intermediate values of $\Delta\beta$ (in this case $\Delta\beta = 1^o$) resulting in infrequent interpolation yielded substantially different dynamics than

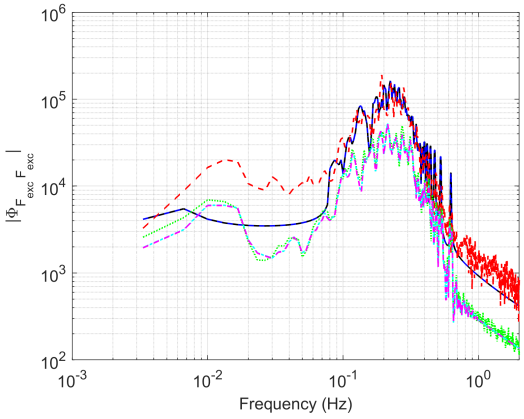

FIGURE 10. AMPLITUDE SPECTRA OF YAW EXCITATION LOAD WITH AND WITHOUT PASSIVE YAW IMPLEMENTATION FOR SEVERAL VALUES OF $\Delta\beta$ UNDER IRREGULAR WAVE EXCITATION. COLORS MAP IN THE SAME MANNER AS FIGURE 7.

smaller values and poorer statistical estimates than runs without interpolation. The ideal value of $\Delta\beta$ will depend additionally on the device under consideration, but a reasonable estimate could likely be made by inspecting a plot of excitation coefficients as a function of relative yaw angle at excited frequencies, like that in Figure 3. If f_{exc} is a strong function of β, smaller values of $\Delta\beta$ will be necessary. Finally, in all cases with irregular waves, multiple phase realizations should be attempted to understand the possible characteristics of time-domain behavior to advise the selection of appropriate values of $\Delta\beta$.

CONCLUSION

The implementation of passive yaw in WEC-Sim allows the accurate modeling of WEC devices for which wave excitation is a strong function of yaw angle. Effective use of this code update requires estimates of excitation coefficients over the range of observed yaw angles at a resolution sufficient to resolve the features of the yaw-dependent excitation. These pre-calculated estimates form the basis for an interpolation of excitation coefficients at time-varying yaw positions. To avoid exorbitant computation times that do not offer commensurate increases in modeling accuracy, it is necessary to prescribe a minimal yaw disturbance $\Delta\beta$ above which interpolation is performed that is non-zero but sufficiently small to capture the important variations in excitation coefficients with yaw. Ideal values of this parameter are likely to be device- and study-specific, but inspecting the gradients of excitation coefficients over yaw angles for excited frequencies offers insight. Further, because time-domain behavior is a convolution involving all previous f_{exc} coefficients, except very small values of $\Delta\beta$, variations in $\Delta\beta$ or other simulation parameters (e.g., the wave ramp time) can cause large variations in time-domain results. However, the results are expected to be representative of actual device physics in the frequency domain and in a statistical sense for sufficiently small selections of $\Delta\beta$, provided estimates of excitation coefficients are available over the range of observed yaw angles. An iterative selection of $\Delta\beta$ that, for irregular waves, involves multiple phase realizations is recommended.

ACKNOWLEDGMENT

Sandia National Laboratories is a multi-mission laboratory managed and operated by National Technology and Engineering Solutions of Sandia, LLC., a wholly owned subsidiary of Honeywell International, Inc., for the U.S. Department of Energy's National Nuclear Security Administration under contract DE-NA0003525. This paper describes objective technical results and analysis. Any subjective views or opinions that might be expressed in the paper do not necessarily represent the views of the U.S. Department of Energy or the United States Government. This work was authored [in part] by the National Renewable Energy Laboratory, operated by Alliance for Sustainable Energy, LLC, for the U.S. Department of Energy (DOE) under Contract No. DE-AC36-08GO28308. Funding provided by the U.S. Department of Energy Office of Energy Efficiency and Renewable Energy Water Power Technologies Office. The views expressed in the article do not necessarily represent the views of the DOE or the U.S. Government. The U.S. Government retains and the publisher, by accepting the article for publication, acknowledges that the U.S. Government retains a nonexclusive, paid-up, irrevocable, worldwide license to publish or reproduce the published form of this work, or allow others to do so, for U.S. Government purposes.

REFERENCES

[1] WEC-Sim (Wave Energy Converter SIMulator) Website.

[2] Tom, N., Ruehl, K., and Ferri, F., 2018. "Numerical model development and validation for the wecccomp control competition". In Proceedings of the 37th International Conference on Offshore Mechanics and Arctic Engineering - OMAE, Vol. 10.

[3] Ruehl, K., Forbush, D. D., Yu, Y. H., and Tom, N., 2020. "Experimental and numerical comparisons of a dual-flap floating oscillating surge wave energy converter in regular waves". *Ocean Engineering,* ***196***(May 2018), p. 106575.

[4] Wendt, F., Nielsen, K., Yu, Y.-h., Bingham, H., Eskilsson, C., Kramer, B., Babarit, A., Bunnik, T., Costello, R., Crowley, S., Giorgi, G., Giorgi, S., Girardin, S., and Greaves, D., 2019. "OES Wave Energy Modelling Task : Modelling , Verification and Validation of Wave Energy Converters". *Journal of Marine Science Engineering*, pp. 1–23.

[5] Tom, N., Lawson, M., and Yu, Y. H., 2015. "Demonstration of the recent additions in modeling capabilities for the WEC-Sim wave energy converter design tool". In Proceedings of the International Conference on Offshore Mechanics and Arctic Engineering - OMAE, Vol. 9.

[6] Lawson, M., Yu, Y. H., Nelessen, A., Ruehl, K., and Michelen, C., 2014. "Implementing nonlinear buoyancy and excitation forces in the WEC-SIM wave energy converter modeling tool". In Proceedings of the 33rd International Conference on Offshore Mechanics and Arctic Engineering - OMAE, no. May.

[7] Ling, B. A., 2019. "Development of a Model Predictive Controller for the Wave Energy Converter Control Competition". In Proceedings of the ASME 2019 38th International Conference on Ocean, Offshore, and Arctic Engineering, pp. 1–10.

[8] Ferri, F., Tom, N., Bacelli, G., Ruehl, K., and Coe, R. G., 2019. "The WECCOMP Wave Energy Competition: Overview". In Proceedings of the 38th International Conference on Ocean, Offshore, and Arctic Engineering.

[9] Tona, P., Sabiron, G., and Nguyen, H.-N., 2019. "An Energy-Maximising MPC Solution To the WEC Control Competition". In Proceedings of the ASME 2018 38th International Conference on Ocean, Offshore and Arctic Engineering, pp. 1–10.

[10] Windt, C., Davidson, J., and Ringwood, J. V., 2018. "High-fidelity numerical modelling of ocean wave energy systems: A review of computational fluid dynamics-based numerical wave tanks". *Renewable and Sustainable Energy Reviews,* ***93***(April), pp. 610–630.

[11] Cummins, W. E., 1962. "The Impulse Response Function and Ship Motions". pp. 101–109.

[12] Yu, Y.-H., Jenne, D., Thresher, R., Copping, A., Geerlofs, S., and Hanna, L., 2015. "Reference Model 5 (RM5): Oscillating Surge Wave Energy Converter". *NREL Technical Report*.

[13] Lee, C.-H., and Newman, J. N., 2017. WAMIT.

[14] Alvez, J. H. G. M., Banner, M. L., and Young, I. R., 2003-7. "Revisiting the pierson-moskowitz asymptoric limits for fully developed wind waves". pp. 1–23.